Food Hydrocolloids xxx (2013) 1–9

Contents lists available at SciVerse ScienceDirect

Food Hydrocolloids

journal homepage: www.elsevier.com/locate/foodhyd

Preparation and characterization of montmorillonite/brea gum nanocomposites films

Aníbal M. Slavutsky [a,*], María A. Bertuzzi [b], Margarita Armada [b], María G. García [c], Nelio A. Ochoa [c]

[a] Agencia Nacional de Promoción Científica y Tecnológica (ANPCyT), Instituto de Investigaciones para la Industria Química (CONICET), CIUNSa, Universidad Nacional de Salta, Av. Bolivia 5150, A4408TVY Salta, Argentina
[b] Instituto de Investigaciones para la Industria Química (CONICET), CIUNSa, Facultad de Ingeniería, Universidad Nacional de Salta, Av. Bolivia 5150, A4408TVY Salta, Argentina
[c] Instituto de Física Aplicada (CONICET), Universidad Nacional de San Luis, Chacabuco 917, San Luis, Argentina

ARTICLE INFO

Article history:
Received 8 June 2012
Accepted 9 June 2013

Keywords:
Edible films
Brea gum
Montmorillonite
Physicochemical properties
Functional properties

ABSTRACT

The aim of this study was the formulation and characterization of films, based on gum exudates from Brea tree and nanoclay particles, for food applications. Brea gum (BG) is a renewable resource available in semi-desert areas. Functional properties of brea gum based films were improved through the incorporation of montmorillonite (MMT). Studies on film forming solution of BG/MMT were conducted. Results indicated a reduction of foam forming with MMT incorporation due to the increase in surface energy. Nanoclay was incorporated to the polymer matrix and films were formed by casting. Effect of nanoclay concentration on physicochemical properties of films was studied. FTIR spectra showed a strong interaction between MMT and BG molecules and X-Ray diffractograms indicated an exfoliated MMT dispersion into film matrix. Optical properties of films were dependent on nanoclay concentration. Solubility and water and gas permeabilities decreased with increasing MMT content. Moisture sorption isotherms of BG and BG/MMT films were obtained. Results indicated that nanoclay incorporation produces a decrease in water uptake of BG. Nanoclay addition produced an increase in Young's module and tensile strength and a decrease in film elongation. Results showed that incorporation of 5% of MMT improved water resistance and water and gas barrier properties of BG based films and enhanced mechanical resistance of these films. Gas permeability measurements indicated that MMT addition reduced permselectivity (CO_2/O_2) of BG film.

© 2013 Elsevier Ltd. All rights reserved.

1. Introduction

For centuries man has searched effective substitutes for natural coating of food to keep them fresh isolated from physical, chemical and/or microbiological contaminants. For many years, the industry of packaging has used materials produced from various petroleum-derived monomers to elaborate varieties of plastics, which have very good functional properties but also produce serious pollution problems. Thanks to advances in science and the growing interest in the environmental impact of discarded plastics, it was developed a new series of materials of biological origin (plant, animal and microbial), whose main advantage is that they are renewable, fully degradable and even edible in some cases. Edible films and coatings generate a modified atmosphere by creating a semi-permeable barrier against O_2, CO_2, moisture and solute movement, thus reducing respiration, water loss and oxidation reaction rates (Martínez-Romero et al., 2006). Various compounds have been used as edible films and coatings, like lipids, proteins and carbohydrates. Proteins and carbohydrates have good mechanical properties and barrier properties against O_2 and CO_2. However, the main functional properties (mechanical and barrier properties) of these hydrophilic materials depend on their water content. This is due to water vapour strongly interacts with polymer matrix affecting the structure (Bertuzzi, Castro Vidaurre, Armada & Gottifredi, 2007; Perdomo et al., 2009). In order to overpass this problem, many attempts have been done like introducing lipids as microdroplets inside the film matrix (Debeaufort, Quezada Gallo, Delporte, & Voilley, 2000; Zahedi, Ghanbarzadeh, & Sedaghat, 2010), incorporation of nanofiller of organic or inorganic origin (Bodirlau, Teaca, &

* Corresponding author. Instituto de Investigaciones para la Industria Química (CONICET), CIUNSa, Universidad Nacional de Salta, Av. Bolivia 5150, A4408TVY Salta, Argentina. Tel.: +54 387 4255410; fax: +54 387 4251006.
E-mail address: amslavutsky@gmail.com (A.M. Slavutsky).

0268-005X/$ – see front matter © 2013 Elsevier Ltd. All rights reserved.
http://dx.doi.org/10.1016/j.foodhyd.2013.06.008

Please cite this article in press as: Slavutsky, A. M., et al., Preparation and characterization of montmorillonite/brea gum nanocomposites films, *Food Hydrocolloids* (2013), http://dx.doi.org/10.1016/j.foodhyd.2013.06.008

Spiridon, 2013; Kampeerapappun, Aht-ong, Pentrakoon, & Srikulkit, 2007) and producing laminated films that consist in a thin lipid layer on the polysaccharide film (Debeaufort et al., 2000; Phan The, Debeaufort, Luu, & Voilley, 2008).

Polysaccharide gums represent one of the most abundant raw materials. Researchers have mainly studied polysaccharide gums due to their sustainable, biodegradable and bio-safe characteristics. The term "gum" is used to describe a group of naturally occurring polysaccharides that come across widespread industrial applications due to their ability either to form gel or make viscous solution or stabilize emulsion systems. The considerably growing interest in plant gum exudates is due to their diverse structural properties and metabolic functions in food, pharmaceutical, cosmetic, textile and biomedical products (Mirhosseini & Amid, 2012).

Brea gum (BG) is the exudate obtained from the Brea tree (*Cercidium praecox*). The gum is harvested from wild trees throughout the northwest region of Argentina by native population (Chane, Wichis and Churupies). BG is a complex hydrocolloids formed by L-arabinose, D-xylose, D-glucuronic acid, and 4-O-methyl-D-glucuronic acid and approximate 8% of protein. The major structural features of BG appear to be a β(1,4)-linked D-xylan backbone (possibly containing some 1,2-linkages) that is heavily 2-substituted by short branched-chains containing residues of D-xylose (and L-arabinose) and D-glucuronic acid, in which both types of residue may be terminal (Cerezo, Stacey, & Webber, 1969). Toxicological studies indicated that BG is not toxic for human ingest (Von Müller, López, Eynard, Aldo & Guzmán, 2009) and it is approved as food additive in Argentine. Physicochemical characteristics of BG are similar to Arabic gum (Bertuzzi, Slavutsky, & Armada, 2012), and then BG can be used as a replacement for Arabic gum in many applications. The easy access to this inexpensive, non-toxic, hydrophilic, biocompatible and biodegradable polysaccharide makes viable its potential use as film matrix for different applications. The development of applications from this natural product and their use at the production zone, for example, to increase the fruit shelf life, might be an important contribution for the local economy.

Many authors formulated edible film and coating using different gums with or without addition of substances like lipids, waxes or polysaccharides to improve their mechanical and water barrier properties (Ali, Maqbool, Ramachandran, & Alderson, 2010; Bosquez-Molina, Guerrero-Legarreta, & Vernon-Carter, 2003; Rojas-Argudo, del Río, & Pérez-Gago, 2009; Ruíz-Ramos et al., 2006). Nanocomposites are hybrid nanostructured materials. A widely studied type of nanocomposite is a class of hybrid materials composed of organic polymer matrices and nanoclay fillers. The essential nanoclay raw material is montmorillonite (MMT), a 2:1 layered smectite clay mineral with a platelet structure. MMT consists in 1 nm thick aluminosilicate layers surface-substituted with metal cations and stacked in 10 μm-sized multilayer stacks. Naturally occurring MMT is hydrophilic (Alexandre & Dubois, 2000).

The introduction of organic or inorganic fillers into a polymeric matrix increases its strength and stiffness and sometimes creates special properties, originating from the synergetic effect between the component materials (Tjong, 2006). Different authors have researched about the use of MMT to improve the characteristics of edible films (Almasi, Ghanbarzadeh, & Entezami, 2010; Chivrac, Pollet, Dole, & Avérous 2010; Tang, Alavi, & Herald, 2008). Tunç and Duman (2010) reported that water adsorption and water solubility decreased as nanoclay concentration increased within the film matrix. Water vapour and gas permeability are also reduced due to the interruption in the diffusion path created by filler particles distributed in the polymeric matrix (Tang et al., 2008). To the best of our knowledge, the use of nanocomposites with plant gums exudates has not been reported in the literature.

The scope of this contribution was to improve water resistance and barrier properties as well as mechanical properties of BG films through the incorporation of nanoclay using an appropriate methodology that ensures adequate exfoliation of the MMT layers within the film matrix.

2. Materials and methods

2.1. Materials

BG was donated from a native community group who live in the production zone of Brea tree (Tartagal, Salta, Argentine). The BG exudate from the plant is collected in the form of small drops or tears. The purification process included the steps of grinding, dissolution, decantation, filtration and drying in oven at temperatures below 50 °C, then grinding to fine powder (mesh 80-ASTM). Humidity of BG powder was 13.5 ± 0.5%, ash 3.8 ± 0.3%, calcium 1.1 ± 0.1%, magnesium 0.3 ± 0.1% and the nitrogen content was 0.95 ± 0.37%. The pH of BG aqueous solutions was 4.7. Natural sodium montmorillonite without purification and with quartz and albite present as accessory minerals, with a cation exchange capacity (CEC) of 89.8 meq/100 g clay, was supplied by Minarco S.A. (Buenos Aires, Argentine). Samples were homogenized by sieving in 200-mesh (ASTM). P_2O_5 (Mallinckrodt, USA) was used as a desiccant. Glycerol (Mallinckrodt, USA) was added as film plasticizer. All salts used to obtain different relative humidity ambient (% RH) were provided by Aldrich (USA).

2.2. Preparation of MMT solution

MMT solution was prepared stirring nanoclay and water (1.5% w/v) during 3 h at 80 °C. The suspension was centrifuged at 2500 rpm. Insoluble matter was rejected. The larger particles or aggregates of nanoclay constituted the precipitate. Smaller particles of MMT remained in colloidal solution and they were separated in the liquid phase from particles of greater size. Centrifugation was used as a selective method of separation. MMT concentration in MMT solution was determined by drying to constant weight, 20 mL aliquot in an oven at 105 °C.

2.3. Film preparation

Film-forming solution was prepared by mixing BG (10% w/v), glycerol in a concentration of 25% w/w of BG, water and the addition of an appropriate amount of MMT solution (prepared as was described in 2.2) to obtain a MMT concentrations ranged from 1 to 5% w/w of BG. The resulting dispersion was kept 60 min in an ultrasonic bath. The pH of film forming solution was not affected by the incorporation of MMT solution. Film forming solution was poured onto polystyrene plates. Then, they were placed in an air-circulating oven at 35 °C and 53% RH for 15 h. After that, plates were removed from the oven and films peeled off. Films were storage at 25 °C and 53% RH before characterization. MMT concentration in films was confirmed through ash content (AOAC, 2003) of BG and BG/MMT films. Analyses were carried out at 800 °C for 4 h and test was done in triplicate for each sample.

2.4. Surface tension and foam capacity of BG/MMT solutions

Surface tension of BG/MMT solutions was measured using Du Noüy ring tensiometer (Krüss Hamburg, Germany) with platinum ring at fixed temperature (25 °C). The method involves slowly lifting a platinum ring from the solution surface. The force required to raise the ring from the liquid surface is measured and related to

Please cite this article in press as: Slavutsky, A. M., et al., Preparation and characterization of montmorillonite/brea gum nanocomposites films, *Food Hydrocolloids* (2013), http://dx.doi.org/10.1016/j.foodhyd.2013.06.008

the solution surface tension. All data were average of at least three measurements.

Solutions of BG/MMT were prepared by mixing BG and MMT solution, elaborated as described in item 2.2. BG concentration was maintained in a constant value of 10% and MMT concentration was varied between 0 and 5%. The solution was transferred to graduate tubes and shacked for 5 min in a Virtis homogenizer (Gardiner, New York). The rotor speed was adjusted at 5000 rpm. Air incorporation was evaluated through tube graduation. The foam capacity (FC) was calculated as follow:

$$\%\,\mathrm{FC} = \frac{\text{Foam volumen}}{\text{Initial Volumen of solution}} \times 100 \quad (1)$$

Measurements were taken at 20 °C. Test was carried out in triplicate for each solution.

2.5. X-ray diffraction, transmission electron microscopy (TEM) and Fourier transformed infra red spectroscopy (FTIR)

X-ray diffraction spectra were carried out on a diffractometer Rigaku MiniFlex (Japan), using a Cu kα radiation, 40 kV and 20 mA over an angular range 1–40° with step size 0.02. Samples were previously conditioned at 53% RH and 25 °C.

Nanostructure of GB/MMT was studied using TEM. The samples for TEM analysis were prepared by blocking the film samples in epoxy resin. Then, the cured epoxies containing the films were microtomed by Leika LKB 2088 model ultramicrotomy. Samples were collected in cupper grid of 200 meshes. TEM micrographs of film samples were obtained by Jeol JSM 100CX II TEM.

IR spectra were obtained using a Perkin Elmer FT-IR spectrometer, GX model (USA). The wave ranged from 4000 to 800 cm^{-1}. Each sample was scanned 40 times for spectrum integration. The scanning resolution was 2 cm^{-1}. The samples were freeze-dried (Thermovac Industries Corp, USA) and stored in a desiccator with P_2O_5 during 48 h. KBr tablets were formed in relation 1:10.

2.6. Thermal gravimetric analysis (TGA)

Thermo gravimetric analyses of BG films and BG/MMT films with 5% of MMT content were obtained. Previously, all films were conditioned at 25 °C and 53% of relative humidity. TGA were performed on a Rigaku Thermoflex 8110 with a TAS 100 Thermogravimetric Analyser (Japan). Samples (10–20 mg) were placed in a platinum crucible and heated from 20 to 1000 °C at a rate of 20 °C/min. Test was carried out in triplicate for each film.

2.7. Optical properties of films

Opacity of films was determined according Gontard, Guilbert, and Cuq (1992) procedure and ASTM D1003 (ASTM, 2011) recommendations. Films prepared with different MMT concentrations were studied. Film samples were cut into rectangles and placed on internal side of the spectrophotometer cell. The absorbance spectrum (400–800 nm) was recorded for each sample using a Spectronic Unicam Genesys 10UV (USA) spectrophotometer. Film opacity was defined as the area under the recorded curve determined by an integration procedure. The opacity was expressed as Absorbance Units × nanometers (AU nm). Samples were previously conditioned at 53% RH and 25 °C.

In the CIE Lab system, colour is represented by three dimensions: L^* related to lightness varied from black (zero) to white (100), and other two related to chromaticity, a^* from green ($-a^*$) to red ($+a^*$) and b^* from blue ($-b^*$) to yellow ($+b^*$). The CIE (Commission Internationale de l'Eclairage) L^*, a^*, b^* colour characteristics were determined using a ColorTec, PCM colorimeter (Accuracy Microsensor Inc., Pittsford, USA), equipped with light source D65 and observation angle 10°. Samples were previously conditioned at 53% RH and 25 °C and measurements were taken at 20 °C. L^*, a^* and b^* values were averaged from five readings at each film.

2.8. Film solubility in water

Film solubility in water was measured as percentage of film dry matter solubilized in water during a period of 24 h. Films prepared with different MMT concentration were analyzed. The initial dry matter of each film was obtained after drying film specimens in desiccators containing P_2O_5 during a week. Samples of approximately 100 mg were weighed and immersed in 20 mL distilled water at 30 °C, sealed and agitated. Films not solubilized in water were separated by centrifugation (Sigma 4K10, Germany) at 2500 g and dried at 40 °C to determine remaining dry matter. Tests were performed by triplicate and solubility was calculated as follows (Equation (2)):

$$\text{Solubility}\ (\%) = \left(\frac{\text{Initial dry weight} - \text{Final dry weight}}{\text{Initial dry weight}}\right) \times 100 \quad (2)$$

2.9. Determination of moisture sorption

Constant relative humidity environments were established inside sorbostats, glass jars, using salt solutions. The salts used (LiCl, CH_3COOK, $MgCl_2$, K_2CO_3, $Mg(NO_3)_2$, NaBr, NaCl, KCl) were the different salts recommended by COST-90 project (Spiess & Wolf, 1983), covering a water activity (a_w) range from 0.10 to 0.90. All salts used were analytical grade. Film samples (rectangular strips approximately 2 cm^2 area) were first freeze-dried (Thermovac Industries Corp, USA) and stored in a desiccator with P_2O_5 during 48 h. Samples were weighed and placed on a stainless plastic lattice by holding it on a tripod inside the sorbostats that contain the saturated salt solutions and then the sorbostats were sealed. The sorbostats were kept inside an environmental chamber maintained at constant temperature. Film samples were equilibrated in the sorbostats for 4 days before their weights were recorded. The sample weights were checked during 3 days more. Equilibrium was judged to have been attained when the difference between two consecutive sample weightings was less than 1 mg/g dry solid. Results at equilibrium were reported for each relative humidity as gram water sorbed/100 g dry film. Absorption tests were done in quadruplicate at each a_w at 25 °C.

The data obtained were fitted by BET sorption model, as described by Equation (3):

$$w_e = \frac{w_0 \cdot C \cdot a_w}{(1 - a_w)\cdot(1 + (C-1)a_w)} \quad (3)$$

where w_e is the equilibrium moisture content (g water/100 g dry film), w_0 is the monolayer moisture content (g water/100 g dry film) and C is a temperature dependent adsorption constant.

The quality of the fitting was evaluated through R^2 and mean relative percent error ($\%E$) defined as:

$$\%E = \sum_{n=1}^{n}\left[\left|\frac{w_{e,i} - w_{p,i}}{w_{e,i}}\right|\right] \times \frac{100}{n} \quad (4)$$

where n is the number of data points, ($w_{e,i}$) and ($w_{p,i}$) are experimentally observed and predicted by the model values of the equilibrium moisture content, respectively.

The mean relative percentage error ($\%E$) has been widely adopted throughout the literature to evaluate the goodness of fit of

Please cite this article in press as: Slavutsky, A. M., et al., Preparation and characterization of montmorillonite/brea gum nanocomposites films, *Food Hydrocolloids* (2013), http://dx.doi.org/10.1016/j.foodhyd.2013.06.008

sorption models, a %*E* value below 10% is indicative of a good fit for practical applications (Al-Muhtaseb, McMinn, & Magee, 2004).

2.10. Water vapour permeability (WVP)

The apparatus and methodology described in the ASTM E96 (ASTM, 2010a, 2010b) were used to measure film permeability. Film specimens were conditioned for 48 h in a chamber at 25 °C and 53% relative humidity ($Mg(NO_3)_2$ saturated salt solution) before being analyzed. The films were sealed on cups containing distilled water (%RH = 100). The test cups were placed in a desiccator cabinet maintained at a controlled temperature (25 °C). A desiccant material was used to provide a specific relative humidity of 0% and uniform conditions at all test locations over the specimen were maintained using a fan. Weight loss measurements were taken by continuous weighing of the test cup to the nearest 0.001 g with an electronic scale (Ohaus PA313, USA). Data were transferred to a computer. Weight loss was plotted over time and when steady state (straight line) was reached, 8 h more were registered. Thickness value was the mean value of five measurements and it was used for water vapour permeability calculations. The water vapour transmission rate (WVTR) was calculated from the slope (G) of a linear regression of weight loss versus time and measured water vapour permeability (WVP) was calculated according to Equation (5):

$$\mathrm{WVP} = \frac{G \cdot l}{A \cdot \Delta p} \tag{5}$$

where l is the film thickness; A is the area of exposed film and Δp is the differential water vapour partial pressure across the film calculated from the difference between the water partial pressure of pure water and that of the desiccant at the experimental temperature. Test was carried out in triplicate for each film.

2.11. Mechanical properties

The tensile properties were measured using a texturometer Brookfield (USA) according to ASTM D882 (ASTM, 2010a, 2010b) with some modifications. The films were cut into strips 25.4 mm wide and 120.0 mm long using a sharp scalpel. The ends of the strips were mounted between cardboard grips using double-side adhesive tape. The final film area exposed was 25.4 mm × 100.0 mm. The texturometer was set to tensile mode. Initial grip separation was 100 mm. Force and elongation was recorded during extension at 20 mm/min up to break. All film strips were equilibrated during a week in a cabinet conditioned at 25 °C and 53% relative humidity using saturated magnesium nitrate solution previous tension assay. Tensile strength (TS), percentage of elongation at break (%*E*) and Young's module of films were evaluated after storage. Test was carried out in triplicate for each film.

2.12. Gas permeation

Gas permeation of Oxygen, Carbon Dioxide and Nitrogenous was tested on BG films and BG/MMT films with 5% of MMT content. All films were conditioned at 25 °C and 0% of relative humidity during a week. Permeability was measured using a classical time lag apparatus (Anson, Marchese, Garis, Ochoa, & Pagliero, 2004). The permeation effective membrane area was 11.34 cm^2 and the constant permeate volume was 35.37 cm^3. The gas permeation measurements were carried out after the system was degassed. It required high vacuum ($p \approx 10^{-4}$ torr) at $T = 30$ °C, during 2 h to ensure that films humidities were 0% RH and to obtain high vacuum at each side of the film. The gas transmitted through the membrane at time t was calculated using the permeate pressure (p_2) readings in the low-pressure side of permeation cell. Permeability coefficients (P) were obtained from the flow rate into the downstream volume upon reaching the steady state as:

$$P = \frac{B \cdot l}{T_c \cdot p_1} \cdot \frac{\mathrm{d}p_2}{\mathrm{d}t} \tag{6}$$

where $B = 11.53$ (cm^3(STP) K)/(cm^2 cmHg) is the cell constant; p_1 (cmHg) is the pressure in the high-pressure side; l (cm) is the membrane thickness; dp_2/dt (cmHg/s) is the slope of the p_2 vs. t plot in steady state and T_c (K) is the temperature of the permeation cell. The linear regression of p_2 vs. t allowed to determine the time elapsed until the steady state conditions have been reached. Films permselectivity or theoretical separation factor (α) was calculated from the relation between carbon dioxide and oxygen permeabilities of each kind of films tested, as follows:

$$\alpha_{CO_2/O_2} = \frac{P_{CO_2}}{P_{O_2}} \tag{7}$$

where P_{CO_2} is the carbon dioxide permeability and P_{O_2} is the oxygen permeability. Permeability coefficients were obtained by the averaging of the values attained from three samples of each membrane and the standard deviation was calculated.

2.13. Statistical analysis

Statistics on a completely randomized design were performed with the analysis of variance (ANOVA) procedure in GraphPad Prism 5.01 software. Tukey's multiple range test ($p \leq 0.05$) was used to detect differences among mean values of films properties.

3. Results and discussion

A biodegradable film based on a nanocomposite formed with BG and MMT plasticized with glycerol, was elaborated. Due to the hydrophilic nature of both, BG and MMT, an enhanced nanodispersion state was expected. Ash content determinations indicated that MMT content in BG/MMT films was 1.03 ± 0.13, 2.97 ± 0.15 and 4.95 ± 0.11 g/100 g of BG, for samples denominated 1, 3 and 5% of MMT, respectively.

3.1. Surface tension and foam capacity of BG/MMT solutions

The behaviour of BG/MMT solution was studied through surface tension and foam capacity as a way of detecting changes in their interfacial properties. These parameters were evaluated as a function of MMT content and they are presented in Table 1. Table 1 also shows surface tension of pure water and MMT solution prepared following the procedure described in 2.2 Section.

The foam formation is a problem in the film elaboration process. Foam cells present in the solution generate pinholes or pores in the film matrix. Due to that, the knowledge of this characteristic is essential for the film final structure.

Table 1
Surface properties of BG/MMT solutions.

MMT content (%)	Foam capacity (%)	Surface tension (mN m^{-1})
0	51.86 ± 3.33	51.75 ± 0.35
1	51.77 ± 3.92	53.70 ± 0.28
3	30.42 ± 4.12	56.6 ± 0.14
5	14.58 ± 2.95	62.15 ± 0.35
MMT solution (0.4%)	–	56.15 ± 0.64
Water	–	69.97 ± 0.18

Please cite this article in press as: Slavutsky, A. M., et al., Preparation and characterization of montmorillonite/brea gum nanocomposites films, *Food Hydrocolloids* (2013), http://dx.doi.org/10.1016/j.foodhyd.2013.06.008

In a previous work, it was reported that surface tension of pure water measured at 25 °C decreased from 69.97 to 51.75 mN m^{-1} when BG concentration reached 5%. It was found that at higher BG concentrations, surface tension remained practically unaltered, indicating that critical micelle concentration was reached at 5% of BG (Bertuzzi et al., 2012). In this work, BG concentration was maintained in a constant value of 10% and the influence of MMT on surface properties of BG solution was study by adding MMT, in concentrations that ranged between 0 and 5%. Results obtained indicate that reduction in FC of BG/MMT solutions is due to an increase in surface tension of BG solutions caused by increasing MMT content.

BG has small quantities of proteins in its composition, attested by a nitrogen content of 0.95%. It is recognized that both protein and particles may be present in many systems, and furthermore, that protein may often be considered as surface active nanoparticles within such system. Thus there may be competitive adsorption between particles and proteins leading to antagonistic or synergistic effect on foam stability (Murray & Ettelaie, 2004). When BG/MMT solution was shaken and aged, the formation of a stable gel was observed. This gel consists in a three-dimensional structure capable of capturing water in its interior. These results provide evidence about the capacity of MMT to interact with the polymeric matrix and they prove that a structure more resistant and stable was formed in the film. Zhang, Sun, Dong, Li and Xu (2008), found a synergistic effect with a surfactant nonionic and laponite, and an antagonistic effect using silica in concentrations lower than 8%.

3.2. X-ray diffraction, transmission electron microscopy (TEM) and FTIR spectra

X-ray diffractograms were performed on MMT powder, BG films and BG/MMT composite films (Fig. 1). X-ray analyses were carried out on the BG/MMT films to investigate the dispersion feature of MMT layers. XRD patterns of BG film samples do not produce sharp diffraction peaks. This indicates that matrix of BG film has no crystalline structure and it is completely amorphous. Similar results were found in arabic gum by Malik, Gupta, and Sarkar (2002) and by Thimma Reddy and Shekharam (2004) in guar gum. MMT pattern displays an intense diffraction peak at 7.06° 2θ angle corresponding to the clay inter-layer spacing value of 1.251 nm. Müller, Borges, and Yamashita (2011) obtained similar X-ray diffraction analyses for MMT.

XRD pattern of BG/MMT film shows that the diffraction peak at 7.06° 2θ angle of MMT disappears. This is indicative of an adequate dispersion of the nanoclay with a high degree of exfoliated morphology in the BG matrix. Huang, Yu, and Ma (2006) obtained similar results with starch/nanoclay composites. These results confirmed that the MMT incorporation is suitable for obtaining exfoliate nanocomposites. MMT was previously diluted in water in order to favour the separation of clay platelets and then mixed with BG. This ensured the formation of an exfoliated nanocomposite in the film matrix. In a previous work about starch/MMT films, it was showed that the group of peaks around 20° also disappears up to a MMT concentration of 7% when the MMT is in an exfoliated manner and 3% when MMT is in an intercalated dispersion within the film matrix (Slavutsky, Bertuzzi, & Armada, 2012). It could be interpreted as a lack in sensitivity of the technique due to the MMT dispersion and dilution in the polymeric matrix.

TEM analysis is a complementary technique of XRD to characterize the nanocomposite structures. TEM micrograph of GB/MMT composite films containing 5% of MMT, which was magnified 140 thousand times, is presented in Fig. 2. The white areas are BG phase and the black areas are the MMT layers dispersed in BG phase. The montmorillonite layers are expanded and homogeneously dispersed in the BG phase at nanometric scale. This TEM observation is consistent with result of XRD analyses. The results obtained from XRD analyses and TEM micrographs confirm that methodology used to incorporate MMT is a suitable method for preparation of exfoliated BG/MMT nanocomposite film. The photographs obtained, provide the information necessary to substantiate the hypothesis that the addition of MMT in films leads to the formation of a tortuous path. The tortuous path formed, is capable of reducing the diffusion rate of molecules through the film, producing a decrease of water permeability.

Relevant zones of FTIR spectrum of MMT, BG and BG/MMT film with 5% MMT are shown in Fig. 3. Typical bands of MMT are found and they are coincident with those reported by Cole (2008) and Xiong, Tang, Tang, and Zou (2007). The wide absorption band at 3432 cm^{-1} indicates the presence of a large number of O—H groups, and the band at 3621 cm^{-1} indicates free O—H groups present in MMT. The maximal absorption at 1093 cm^{-1} is attributed to stretching and flexural vibration of Si—O—Si. It has been reported that structural features of brea gum is a b-(1→4)-linked D-xylan backbone substituted by short branch-chains containing residues of D-xylose (and L-arabinose) and D-glucoronic acid, in which both types of residues may be terminal (Cerezo et al., 1969; De Pinto, Martínez, & Rivas, 1994). BG spectrum confirms the reported structure and shows a strong band at 3426 cm^{-1} concerned with —OH groups.

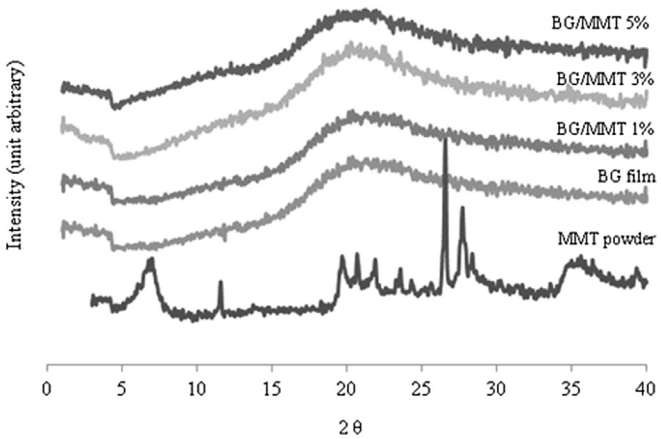

Fig. 1. X-ray diffractograms of BG, BG/MMT films and MMT powder.

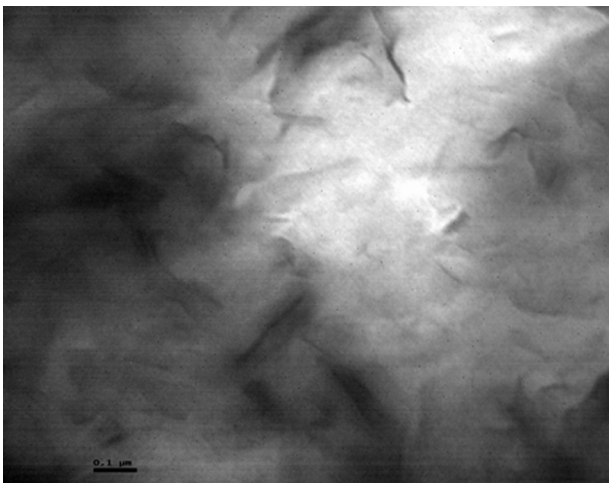

Fig. 2. TEM micrograph of BG/MMT films (5% MMT).

Please cite this article in press as: Slavutsky, A. M., et al., Preparation and characterization of montmorillonite/brea gum nanocomposites films, *Food Hydrocolloids* (2013), http://dx.doi.org/10.1016/j.foodhyd.2013.06.008

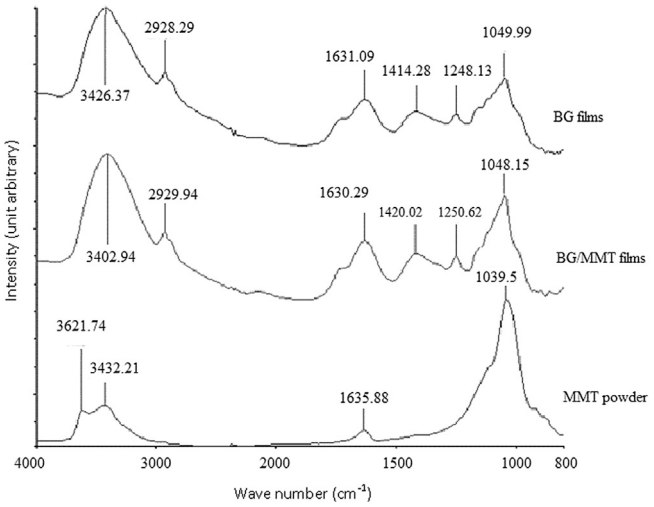

Fig. 3. FT-IR spectra of MMT powder and BG and BG/MMT film (5% MMT).

Other band is observed at 2928 cm^{-1} corresponding to stretching vibration of C—H bond; the bands at 1631 and 1414 cm^{-1} are assigned to asymmetric and symmetric vibration of the carboxylic acid salt $-COO^-$ of D-glucuronic acid, and 4-O-methyl-D-glucuronic acid and bands at 1248 and 1049 cm^{-1} due to the stretching of the C—O bond. Espinosa-Andrews, Sandoval-Castilla, Vasquez-Torres, Vernon-Carter and Lobato-Calleros (2010) obtained similar IR spectra for Arabic gum.

In the O—H stretching vibration region at 3000–3600 cm^{-1}, it is observed a shift to lower wavenumber in the characteristic peak of BG when MMT is added in the film matrix. It is indicative of a strong interaction between BG chains and MMT through hydrogen bonds. This indicates that in the BG/MMT nanocomposite, hydrogen bonds between BG chains are broken and new hydrogen bonds between the hydroxyl groups of MMT and hydroxyl groups of BG molecules are formed. The disappearance of band at 3621 cm^{-1} in MMT spectra was reported by other authors, indicating the replacement of water molecules in the interlayer of MMT and the formation of new hydrogen bonds with the polymer (Cyras, Manfredi, Tom-That, & Vásquez, 2008; Liu, Chaudhary, Yusa, & Tadé, 2011). Moreover C—O band at 1049 cm^{-1} shows not only a little shift to 1048 cm^{-1} but also a most intense band indicating a higher hydrogen bond formation between C—O and Si—O—Si groups indicating that ring structure of D-xylan backbone is affected by the additions of MMT (Wang & Sain, 2007).

3.3. Thermal gravimetric analysis (TGA)

The thermal stability of the plasticized BG-based nanocomposites has been assessed by thermo gravimetric analysis. TGA was performed in order to determine if the addition of clay produces any change on the thermal decomposition behaviour of BG.

Table 2
Thermogravimetric data of BG and BG/MMT at 5% films.

Film	Temperature	First stage (°C)	Second stage (°C)	Third stage (°C)
BG	Initial/Final	13 ± 1/ 240 ± 3	273 ± 3/ 331 ± 2	414 ± 4/ 665 ± 3
	Peak	98 ± 2	302 ± 2	490 ± 3
BG/MMT	Initial/Final	17 ± 2/ 241 ± 2	281 ± 2/ 324 ± 3	427 ± 1/ 670 ± 3
	Peak	102 ± 1	307 ± 2	504 ± 4

TGA results obtained for BG films and BG/MMT films with 5% of MMT are shown in Table 2. The early minor weight loss in samples is attributed to desorption of moisture linked by hydrogen bounds to the polysaccharide structure. The second step corresponds to the glycerol plasticizer volatilization. Chivrac, Pollet, Schmutz and Avérous (2010) obtain similar result in starch/glycerol film. The third weight loss corresponds to the BG thermal degradation. BG presents thermal decomposition at higher temperatures than those obtained by Zohuriaan and Shokrolahi (2004) for different gums.

The peak temperatures of the three stages observed in the BG matrix shifted towards higher temperatures when MMT was introduced in the film matrix. This increase in degradation temperatures is commonly observed in films containing MMT. It is attributed to the increase in tortuosity of the diffusion pathway induced by the clay dispersion, which limits the diffusion of the oxygen and the pyrolysis gases from and to the material surface (García, Hoyos, Guzmán, & Tiemblo, 2009; Ray & Okamoto, 2003). Tunc et al. (2007) obtained similar results in wheat gluten/MMT film. According to Cyras et al. (2008) inorganic materials has better thermal stability than organic materials. The clay acts as a heat barrier, which enhances the overall thermal stability of the composites. Consequently, the incorporation of inorganic particles improves the thermal stability of BG. The increment on peak temperatures obtained in BG/MMT film in all the stages of degradation indicates that MMT present a homogeneous dispersion into BG matrix.

3.4. Optical properties of films

Table 3 shows that opacity of BG/MMT films increases with MMT incorporation. Nanoparticle incorporation produces a decrease in the transparency of films based on amorphous matrix due to change in light diffraction produced by the dispersed particles. Film opacity increases was dependent on the amount of nanoclay incorporated. It was observed that opacity of BG film increased from 120 to 182 AU nm when 5% of MMT was added. Sothornvit, Rhim, and Hong (2009) reported that transmittance of the whey protein isolate film decreased when MMT was incorporated in a concentration of 5%. They found that the decrease was depending on type of MMTs used. They observed that a good dispersion and a high compatibility between polymer and clay particles can enhance gloss and transparency of nanocomposite films based on whey protein isolate. Rhim (2011) studied the transmittance of agar/clay composite films as a function of MMT content between 0 and 20% and he found higher opacities in all the range analyzed.

Table 3 presents colour evaluation parameters of BG/MMT films. Increasing MMT content in BG/MMT films produces slight modifications in L^*, a^* and b^* values. It indicates a decrease in lightening and an increase in yellowness and redness due to the incorporation of MMT. Sothornvit et al. (2009) reported similar trends in whey protein isolate/clay composite films, detecting a decrease in L^* values and an increase in a^* and b^* values due to MMT incorporation.

Table 3
Optical properties of BG/MMT films as function of MMT content.

MMT content (%)	Opacity (AU nm)	Colour		
		L	a^*	b^*
0	120 ± 21	62.09 ± 0.75	5.91 ± 1.05	12.84 ± 1.02
1	160 ± 17	58.66 ± 0.83	5.95 ± 0.87	19.97 ± 1.12
3	175 ± 19	58.12 ± 0.84	7.48 ± 0.96	24.45 ± 0.89
5	182 ± 23	56.75 ± 0.93	8.25 ± 1.04	25.67 ± 1.09

Please cite this article in press as: Slavutsky, A. M., et al., Preparation and characterization of montmorillonite/brea gum nanocomposites films, *Food Hydrocolloids* (2013), http://dx.doi.org/10.1016/j.foodhyd.2013.06.008

3.5. Film solubility in water

Solubility in water is an important property of edible films for food packaging and pharmaceutical applications. Some potential uses may require water insolubility to enhance product integrity and water resistance. However, in other cases, water solubility of the film before product consumption might be useful as in encapsulation of drug, food or additives.

The addition of MMT reduces the film solubility. It was found that film solubility decreases with the increase of MMT content (Table 5). It is indicative of a better interaction between BG chains and MMT in the film, which is facilitated by a better dispersion of the nanoclay into the polymer matrix. Exfoliated structure improves intermolecular interaction between film components. Hydrogen bonds between MMT and hydrocolloid chains are stronger than those formed by the MMT with water or the hydrocolloid with water. As a consequence, film solubility, in the solvent in which was prepared, decreases. Some authors observed similar behaviour in starch/MMT films (Majdzadeh-Ardakani, Navarchian, & Sadeghi, 2010; Ning, Xingxiang, Na, & Shihe, 2009).

3.6. Sorption isotherm

Mechanical and barrier properties of hydrocolloids based films are influenced by relative humidity. Moisture sorption curves were studied to evaluate the storage stability and properties of BG/MMT films. Fig. 4 shows the moisture sorption data and BET model fit of BG/MMT films with different MMT content. The moisture content of samples shows an increase with equilibrium relative humidity. However, equilibrium water content in the film matrix decreases as MMT content increases. The structure of the film is modified above a certain degree of freedom of water. Under these conditions, polymeric chains swell altering its structure. Experimental data obtained for BG/MMT film indicate that incorporation of nanoclay reduces water sorption. This effect increases at high a_w, demonstrating that water has less affinity for the film. MMT is capable to interact with hydrophilic group of BG. These results indicated that the addition of MMT improves the water resistance of the BG matrix, which was attested by results of film solubility and FTIR spectra. Possibly, the strong interactions between BG and hydroxyl groups of the MMT layers, through hydrogen bonds, reduce the number of hydrophilic sites available for water molecules resulting in a decrease of water solubility and diffusivity in the film matrix. As a result, the water sensitivity of a highly hydrophilic composite film was reduced. Water content data for a_w values exceeding 0.75 are not considered due to the high hydrophilicity of BG. The results were in the same range of data reported by Almasi et al. (2010) for starch–carboxymethylcellulose–nanoclay biodegradable films, and by Tunç and Duman (2010) for methyl cellulose-MMT films.

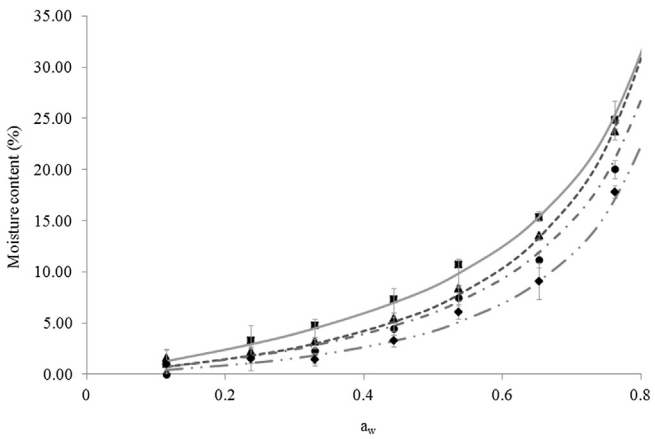

Fig. 4. Moisture sorption isotherms of BG (■) and BG/MMT (1% ▲; 3% ●; 5% ◆) films and BET model (0% ——; 1% – – –; 3% – · –; 5% — · · —). Bars indicate standard deviation.

Table 4
BET model parameters of BG/MMT films as function of MMT content.

MMT content (%)	w_0	C	R^2	%Error
0	8.6271	0.6202	0.9883	1.27
1	7.3566	1.4213	0.9813	1.33
3	7.1594	0.7273	0.9803	2.53
5	6.9123	0.4488	0.9776	2.97

Table 4 shows fitting parameters of BET model. Monolayer water content decreases as MMT content increases as it was determined by BET model parameters. All curves correspond to type III isotherm according to Brunauer classification.

3.7. Water vapour permeability

Permeability depends on the solubility and diffusivity of the water in the polymeric matrix. According to the XRD and FTIR spectra, the greatest interaction between MMT and BG hinders the passage of water molecules through the film. The WVP of BG/MMT films as function of MMT content is showed in Table 5. The addition of MMT nanoparticles results in a significant decrease of WVP regarding the unfilled system. This behaviour is associated with the combined effect of decreasing in water solubility observed in Table 5 and the tortuous path caused by nanoclay incorporation (Fig. 2). Wang, Zhang, and Wang (2009) obtained similar results with modified and unmodified MMT in starch/glycerol films, and attributed the decrease in WVP to the strong interaction of MMT with starch and to the formation of a tortuous path. The same behaviour was reported by Tunc et al. (2007) in films based on wheat gluten and MMT.

3.8. Mechanical properties

Mechanical properties were determined using tensile test and results are shown in Table 5. TS and Young's module increase with MMT content. The increase of Young's module indicates that the film becomes more rigid, resistant to lengthening or stretching, as the MMT content increases. Young's module increases from 392 to 738 MPa and TS increases from 7.45 to 20.96 MPa, with the addition of 5% of MMT. %E decreases from 19.97 to 9.32 when MMT concentration increases from 0 to 5%. The structure of BG and the incorporation technique of MMT nanoparticle generate an appropriate dispersion of nanoclay into the polymeric matrix. It favours the strong interaction between BG and MMT through numerous hydrogen bonds and produces these modifications in mechanical properties due to the high surface area (about 750 m^2/g), high

Table 5
Mechanical and water barrier properties of BG and BG/MMT films.

MMT content (%)	TS[a] (MPa)	Elongation (%)[a]	Young module[a] (MPa)	Solubility (%)[b]	WVP 10.E-10 (g s^{-1} m^{-1} Pa^{-1})[a]
0	7.45 ± 0.43	19.97 ± 1.86	392 ± 27	31.03 ± 1.20	7.17 ± 0.38
1	11.97 ± 0.61	14.96 ± 1.65	474 ± 32	29.0 5 ± 0.97	5.22 ± 0.27
3	14.92 ± 0.58	11.38 ± 0.97	699 ± 19	23.64 ± 0.89	4.41 ± 0.31
5	20.96 ± 0.55	9.31 ± 1.31	738 ± 21	21.11 ± 0.93	3.79 ± 0.23

[a] Sample conditioned at 25 °C and 53% RH.
[b] Analysis conditions 30 °C and 0% RH.

Please cite this article in press as: Slavutsky, A. M., et al., Preparation and characterization of montmorillonite/brea gum nanocomposites films, *Food Hydrocolloids* (2013), http://dx.doi.org/10.1016/j.foodhyd.2013.06.008

Table 6
Gas permeability[a] of BG films and BG/MMT films with 5% of MMT content.

	O_2	N_2	CO_2	CO_2/O_2
BG	2.03E-10 ± 0.05	1.40E-10 ± 0.06	1.89E-10 ± 0.03	0.93 ± 0.01
BG/MMT	1.72E-10 ± 0.06	0.55E-10 ± 0.07	1.00E-10 ± 0.04	0.58 ± 0.01

[a] Gas permeabilities are expressed in Barrer units ($cm^3_{(STP)} \cdot cm \cdot cm^{-2} \cdot s^{-1} \cdot cm_{Hg}^{-1}$). Analysis conditions: 30 °C and 0%RH.

aspect ratio (50–1000), and very high elastic modulus (178 GPa) of the clay (Rhim, 2011). Similar results were also observed by other authors in nanocomposites films (Cyras et al., 2008; Tjong, 2006).

3.9. Gas permeation

Oxygen is the key factor for oxidation, which is responsible for changes in food odour, colour, flavour and nutrients deterioration. Therefore, films that provide a proper oxygen barrier can help in improving food quality and extending food shelf life. Carbon dioxide is very important to the respiration of living tissues and higher values of carbon dioxide can delay fruits softening (Cerqueira, Lima, Teixeira, Moreira, & Vicente, 2009).

Gas permeation results obtained for BG films and BG/MMT films with 5% of MMT are shown in Table 6. Permeation is known to be governed by two mechanisms: diffusion and solution. Solubility depends on hydrophilic or hydrophobic character of gases and diffusivity is related to difficulties in the passage of gas through the membrane. Table 6 shows that the MMT incorporation reduces films permeability of all tested gases, due to the increase in the tortuosity of the gas molecules path through the film matrix caused by nanoclay particles.

Permeability test of BG films indicates that the difference between oxygen and carbon dioxide permeabilities was negligible. Nitrogen resulted less permeable than the other studied gases in both film matrices due to its highest kinetic diameter ($\sigma_{kCO_2} = 3.36$ Å; $\sigma_{kO_2} = 3.46$ Å; $\sigma_{kN_2} = 3.64$ Å). Permselectivity of BG/MMT films indicated an important decrease in carbon dioxide permeability. It can be explained by decreasing in hydrophilicity of the composite film and the tortuous pathway formed by MMT incorporation in spite of the fact that CO_2 has the lowest kinetic diameter. CO_2 is a quadrupolar gas molecule that strongly interacts with polar groups present in the composite film. Polymers containing polar moieties, such as ether groups, have an affinity for CO_2 due to dipole–quadrupole interactions. These gas molecule–polymer interactions favour CO_2 solubility rather than other nonpolar gases. The decrease of oxygen and nitrogen permeability was exclusively dependent on tortuous pathway formed by the incorporation of MMT. Quilaqueo Gutiérrez, Echeverría, Ihl, Bifani, and Mauri (2012) obtained a similar behaviour for oxygen permeability in carboxymethylcellulose/MMT films.

4. Conclusions

The behaviour of BG hydrocolloid and MMT particles in aqueous solution were studied. The incorporation of MMT in film forming solution indicated a strong interaction between BG and MMT. These interactions allowed the formation of a network capable to avoid the formation of foam in film solution. Well developed bionanocomposite films were prepared with BG and different amounts of MMT using a solvent dispersion method. Film properties of the nanocomposite films were influenced by the clay content. The technique used to MMT incorporation provided an exfoliated structure into the film matrix as evidenced by XRD and TEM analyses. Decreases in solubility and water sorption capacity indicated a strong interaction between the functional groups of MMT and BG. The decrease in water vapour permeability with MMT content confirms that a strong interaction between hydrophilic groups of MMT and BG exists and that water molecules move through a tortuous path when diffuse across the polymer matrix. Film opacity increases with MMT addition. MMT incorporation affects mechanical properties of BG/MMT films. The increase of Young's module indicates that the film becomes more rigid, resistant to lengthening or stretching, as the MMT content increases. TS also increases accompanied by a loss of elongation. Gas permeability measurements indicated that MMT addition reduces film permeability to O_2, N_2 and CO_2, but also permselectivity (CO_2/O_2) of BG film is reduced. Nanotechnology provides an alternative technique for the improvement of both barrier and mechanical properties of BG based films. The BG/MMT nanocomposite films with improved water vapour and gas barrier and mechanical properties could be potentially used as environmentally friendly food packaging materials for extending food shelf-life.

Acknowledgement

The authors thank the financial support of Consejo de Investigaciones de la Universidad Nacional de Salta (CIUNSa), Agencia Nacional de Promoción Científica y Tecnológica (ANPCyT) and Instituto de Investigaciones para la Industria Química (INIQUI) and the technical support of Ing. Edgardo Sham with TGA analyses and Cecilia Gutierrez Ayesta with TEM analyses.

References

Alexandre, M., & Dubois, P. (2000). Polymer-layered silicate nanocomposites: preparation, properties and uses of a new class of materials. *Materials Science and Engineering: R: Reports, 28*(1–2), 1–63.

Ali, A., Maqbool, M., Ramachandran, S., & Alderson, P. G. (2010). Gum arabic as a novel edible coating for enhancing shelf-life and improving postharvest quality of tomato (*Solanum lycopersicum* L.) fruit. *Postharvest Biology and Technology, 58*(1), 42–47.

Almasi, H., Ghanbarzadeh, B., & Entezami, A. A. (2010). Physicochemical properties of starch-CMC-nanoclay biodegradable films. *International Journal of Biological Macromolecules, 46*(1), 1–5.

Al-Muhtaseb, A. H., McMinn, W., & Magee, T. (2004). Water sorption isotherm of starch powders: part 1: mathematical description of experimental data. *Journal of Food Engineering, 61*(3), 297–307.

Anson, M., Marchese, J., Garis, E., Ochoa, N. A., & Pagliero, C. (2004). ABS copolymer-activated carbon mixed matrix membranes for CO_2/CH_4 separation. *Journal of Membrane Science, 243*, 19–28.

AOAC. (2003). *Method 923.03. Ash of flour – Direct method* (17th ed.). Official Methods of Analysis of the Association of Official Analytical Chemists International.

ASTM. (2010a). *Standards American society for testing and materials*. D882 Standard test methods for tensile properties of thin plastic sheeting. Philadelphia, USA.

ASTM. (2010b). *Standards American society for testing and materials*. E96. Standard test methods for water vapor transmission of materials. Philadelphia.

ASTM. (2011). *Standards American society for testing and materials*. D1003. Standard test method for haze and luminous transmittance of transparent plastics. Philadelphia, USA.

Bertuzzi, M. A., Castro Vidaurre, E. F., Armada, M., & Gottifredi, J. C. (2007). Water vapor permeability of edible starch based films. *Journal of Food Engineering, 80*(3), 972–978.

Bertuzzi, M. A., Slavutsky, A. M., & Armada, M. (2012). Physicochemical characterisation of the hydrocolloid from Brea tree (*Cercidium praecox*). *International Journal of Food Science & Technology, 47*(4), 768–775.

Bodirlau, R., Teaca, C. A., & Spiridon, J. (2013). Influence of natural fillers on the properties of starch-based biocomposite films. *Composites: Part B, 44*, 575–583.

Bosquez-Molina, E., Guerrero-Legarreta, I., & Vernon-Carter, E. J. (2003). Moisture barrier properties and morphology of mesquite gum-candelilla wax based edible emulsion coatings. *Food Research International, 36*(9–10), 885–893.

Cerezo, A. S., Stacey, M., & Webber, J. M. (1969). Some structural studies of brea gum (an exudate from *Cercidium australe* jonhst.). *Carbohydrate Research, 9*(4), 505–517.

Cerqueira, M. A., Lima, A. M., Teixeira, J. A., Moreira, R. A., & Vicente, A. A. (2009). Suitability of novel galactomannans as edible coatings for tropical fruits. *Journal of Food Engineering, 94*(3–4), 372–378.

Chivrac, F., Pollet, E., Dole, P., & Avérous, L. (2010). Starch-based nanobiocomposites: plasticizer impact on the montmorillonite exfoliation process. *Carbohydrate Polymers, 79*(4), 941–947.

ARTICLE IN PRESS

Chivrac, F., Pollet, E., Schmutz, M., & Avérous, L. (2010b). Starch nano-biocomposites based on needle-like sepiolite clays. *Carbohydrate Polymers, 80*(1), 145–153.
Cole, K. C. (2008). Use of infrared spectroscopy to characterize clay intercalation and exfoliation in polymer nanocomposites. *Macromolecules, 41*, 834–843.
Cyras, V. P., Manfredi, L. B., Ton-That, M.-T., & Vázquez, A. (2008). Physical and mechanical properties of thermoplastic starch/montmorillonite nanocomposite films. *Carbohydrate Polymers, 73*(1), 55–63.
Debeaufort, F., Quezada-Gallo, J. A., Delporte, B., & Voilley, A. (2000). Lipid hydrophobicity and physical state effects on the properties of bilayer edible films. *Journal of Membrane Science, 180*, 47–55.
De Pinto, G. L., Martinez, M., & Rivas, C. (1994). Chemical and spectroscopic studies of *Cercidium praecox* gum exudates. *Carbohydrate Research, 260*, 17–25.
Espinosa-Andrews, H., Sandoval-Castilla, O., Vázquez-Torres, H., Vernon-Carter, E. J., & Lobato-Calleros, C. (2010). Determination of the gum Arabic–chitosan interactions by Fourier Transform Infrared Spectroscopy and characterization of the microstructure and rheological features of their coacervates. *Carbohydrate Polymers, 79*(3), 541–546.
García, N., Hoyos, M., Guzman, J., & Tiemblo, P. (2009). Comparing the effect of nanofillers as thermal stabilizers in low density polyethylene. *Polymer Degradation and Stability, 94*(1), 39–48.
Gontard, N., Guilbert, S., & Cuq, J. L. (1992). Edible wheat gluten films: influence of the main process variables on film properties using response surface methodology. *Journal of Food Science, 57*, 195–199.
Huang, M., Yu, J., & Ma, X. (2006). High mechanical performance MMT-urea and formamide-plasticized thermoplastic cornstarch biodegradable nanocomposites. *Carbohydrate Polymers, 63*, 393–399.
Kampeerapappun, P., Aht-ong, D., Pentrakoon, D., & Srikulkit, K. (2007). Preparation of cassava starch/montmorillonite composite film. *Carbohydrate Polymers, 67*, 155–163.
Liu, H., Chaudhary, D., Yusa, S.-i., & Tadé, M. O. (2011). Glycerol/starch/Na^{+}-montmorillonite nanocomposites: a XRD, FTIR, DSC and ^{1}H NMR study. *Carbohydrate Polymers, 83*(4), 1591–1597.
Majdzadeh-Ardakani, K., Navarchian, A., & Sadeghi, F. (2010). Optimization of mechanical properties of thermoplastic starch/clay nanocomposites. *Carbohydrate Polymers, 79*, 547–554.
Malik, H., Gupta, N., & Sarkar, A. (2002). Anisotropic electrical conduction in gum arabic—a biopolymer. *Materials Science and Engineering C, 20*, 215–218.
Martínez-Romero, D., Alburquerque, N., Valverde, J. M., Guillén, F., Castillo, S., Valero, D., et al. (2006). Postharvest sweet cherry quality and safety maintenance by *Aloe vera* treatment: a new edible coating. *Postharvest Biology and Technology, 39*, 92–100.
Mirhosseini, H., & Amid, B. T. (2012). A review study on chemical composition and molecular structure of newly plant gum exudates and seed gums. *Food Research International, 461*, 387–398.
Müller, C. M. O., Borges, J., & Yamashita, F. (2011). Effect of nanoclay incorporation method on mechanical and water vapor barrier properties of starch-based films. *Industrial Crops and Products, 33*, 605–610.
Murray, B. S., & Ettelaie, R. (2004). Foam stability: proteins and nanoparticles. *Current Opinion in Colloid & Interface Science, 9*(5), 314–320.
Ning, W., Xingxiang, Z., Na, H., & Shihe, B. (2009). Effect of citric acid and processing on the performance of thermoplastic starch/montmorillonite nanocomposites. *Carbohydrate Polymers, 76*(1), 68–73.
Perdomo, J., Cova, A., Sandoval, A., García, L., Laredo, E., & Müller, L. (2009). Glass transition temperatures and water sorption isotherms of cassava starch. *Carbohydrate Polymers, 76*, 305–313.
Phan The, D., Debeaufort, F., Luu, D., & Voilley, A. (2008). Moisture barrier, wetting and mechanical properties of shellac/agar or shellac/cassava starch bilayer biomembrane for food applications. *Journal of Membrane Science, 325*, 277–283.
Quilaqueo Gutiérrez, M., Echeverría, I., Ihl, M., Bifani, V., & Mauri, A. N. (2012). Carboxymethylcellulose–montmorillonite nanocomposite films activated with murta (*Ugni molinae* Turcz) leaves extract. *Carbohydrate Polymers, 87*(2), 1495–1502.
Ray, S., & Okamoto, M. (2003). Polymer/layered silicate nanocomposites: a review from preparation to processing. *Progress in Polymers Science, 28*, 1539–1641.
Rhim, J. (2011). Effect of clay contents on mechanical and water vapor barrier properties of agar-based nanocomposite films. *Carbohydrate Polymers, 86*(2), 691–699.
Rojas-Argudo, C., del Río, M. A., & Pérez-Gago, M. B. (2009). Development and optimization of locust bean gum (LBG)-based edible coatings for postharvest storage of Fortune' mandarins. *Postharvest Biology and Technology, 52*(2), 227–234.
Ruíz-Ramos, J. O., Pérez-Orozco, J. P., Báez-González, J. G., Bósquez-Molina, E., Pérez-Alonso, C., & Vernon-Carter, E. J. (2006). Interrelationship between the viscoelastic properties and effective moisture diffusivity of emulsions with the water vapor permeability of edible films stabilized by mesquite gum-chitosan complexes. *Carbohydrate Polymers, 64*(2), 355–363.
Slavutsky, A. M., Armada, M., & Bertuzzi, M. A. (2012). Water barrier properties of starch-clay nanocomposite films. *Brazilian Journal of Food Technology, 15*(3), 208–218.
Sothornvit, R., Rhim, J.-W., & Hong, S.-I. (2009). Effect of nano-clay type on the physical and antimicrobial properties of whey protein isolate/clay composite films. *Journal of Food Engineering, 91*(3), 468–473.
Spiess, W. E. L., & Wolf, W. F. (1983). *The results of the COST 90 project on water activity*. In *Physical properties of foods*: . London: Applied Science Publishers.
Tang, X., Alavi, S., & Herald, T. H. (2008). Effects of plasticizers on the structure and properties of starch–clay nanocomposite films. *Carbohydrate Polymers, 74*(3), 552–558.
Thimma Reddy, T., & Shekharam, T. (2004). Free radical degradation of guar gum. *Polymer Degradation and Stability, 86*, 455–459.
Tjong, S. C. (2006). Structural and mechanical properties of polymer nanocomposites. *Materials Science and Engineering, 53*, 73–197.
Tunc, S., Angellier, H., Cahyana, Y., Chalier, P., Gontard, N., & Gastaldi, E. (2007). Functional properties of wheat gluten/montmorillonite nanocomposite films processed by casting. *Journal of Membrane Science, 289*, 159–168.
Tunç, S., & Duman, O. (2010). Preparation and characterization of biodegradable methyl cellulose/montmorillonite nanocomposite films. *Applied Clay Science, 48*, 414–424.
Von Müller, A. R., López, C. B., Eynard, B., Aldo, R., & Guzmán, C. A. (2009). Subchronic toxicological evaluation of brea gum (*Parkinsonia preacox*) as a food additive in BALB/c mice. *Drug and Chemical Toxicology, 32*(4), 307–311.
Wang, B., & Sain, M. (2007). Isolation of nanofibers from soybean source and their reinforcing capability on synthetic polymers. *Composites Science and Technology, 67*, 2521–2527.
Wang, W., Zhang, J., & Wang, A. (2009). Preparation and swelling properties of superabsorbent nanocomposites based on natural guar gum and organo-vermiculite. *Applied Clay Science, 46*(1), 21–26.
Xiong, H., Tang, S. W., Tang, H., & Zou, P. (2007). The structure and properties of starch-based biodegradable film. *Carbohydrate Polymers, 71*, 263–268.
Zahedi, Y., Ghanbarzadeh, B., & Sedaghat, N. (2010). Physical properties of edible emulsified films based on pistachio globulin protein and fatty acids. *Journal of Food Engineering, 100*, 102–108.
Zhang, S., Sun, D., Dong, X., Li, C., & Xu, J. (2008). Aqueous foams stabilized with particles and nonionic surfactants. *Colloids and Surfaces A: Physicochemical and Engineering Aspects, 324*(1–3), 1–8.
Zohuriaan, M. J., & Shokrolahi, F. (2004). Thermal studies on natural and modified gums. *Polymer Testing, 23*(5), 575–579.

Please cite this article in press as: Slavutsky, A. M., et al., Preparation and characterization of montmorillonite/brea gum nanocomposites films, *Food Hydrocolloids* (2013), http://dx.doi.org/10.1016/j.foodhyd.2013.06.008